Available online at www.sciencedirect.com
SCIENCE DIRECT
PHYSICS LETTERS B
Physics Letters B 585 (2004) 243–252
www.elsevier.com/locate/physletb

On baryon resonances and chiral symmetry

E.E. Kolomeitsev [a], M.F.M. Lutz [b,c]

[a] The Niels Bohr Institute, Blegdamsvej 17, DK-2100 Copenhagen, Denmark
[b] Gesellschaft für Schwerionenforschung (GSI), Planck Str. 1, 64291 Darmstadt, Germany
[c] Institut für Kernphysik, TU Darmstadt, D-64289 Darmstadt, Germany

Received 30 May 2003; received in revised form 12 December 2003; accepted 11 January 2004

Editor: J.-P. Blaizot

Abstract

We study $J^P = \frac{3}{2}^-$ baryon resonances as generated by chiral coupled-channel dynamics in the χ-BS(3) approach. Parameter-free results are obtained in terms of the Weinberg–Tomozawa term predicting the leading s-wave interaction strength of Goldstone bosons with baryon-decuplet states. In the 'heavy' $SU(3)$ limit with $m_\pi = m_K \sim 500$ MeV the resonances turn into bound states forming a decuplet and octet representation of the $SU(3)$ group. Using physical masses the mass splitting are remarkably close to the empirical pattern.

1. Introduction

In this Letter we further test the conjecture [1–4] that baryon resonances not belonging to the large-N_c ground states may be generated by coupled-channel dynamics [5–10]. In recent works [1,2,11,12] it was shown that chiral dynamics as implemented by the χ-BS(3) approach [1,2,4] provides a parameter-free prediction for the existence of a wealth of s-wave baryon resonances. The latter may be classified in the 'heavy' $SU(3)$ limit as forming two mass-degenerate octet and one singlet states [5–9,12,18]. Related works that adhere a different strategy not insisting on improved crossing-transformation properties and perturbative subthreshold amplitudes are [13–18]. All these findings support our conjecture. In the $SU(6)$ quark-model approach such s-wave resonances belong to a 70-plet, that contains many more resonance states [19]. An interesting question arises: what is the role played by the d-wave resonances belonging to the very same 70-plet as the s-wave resonances studied in [12]. The phenomenological model [3] generated successfully also non-strange d-wave resonances belonging to the 70-plet by coupled-channel dynamics describing a large body of pion and photon scattering data.

Naively one may expect that chiral dynamics does not make firm predictions for d-wave resonances since the meson–baryon interaction in the relevant channels probes a set of counter terms presently unknown. However, this is not necessarily so. Since a d-wave baryon resonance couples to s-wave meson–baryon-decuplet states chiral symmetry is quite predictive for such resonances under the assumption that the latter channels are dominant. This is

E-mail address: m.lutz@gsi.de (M.F.M. Lutz).

doi:10.1016/j.physletb.2004.01.066

in full analogy to the analysis of the s-wave resonances [5–9,11,12,18] that neglects the effect of the contribution of d-wave meson–baryon-decuplet states. The empirical observation that the d-wave resonances $N(1520)$, $N(1700)$ and $\Delta(1700)$ have large branching fractions ($> 50\%$) into the inelastic $N\pi\pi$ channel, even though the elastic πN channel is favored by phase space, supports our assumption. A parameter free scheme arises since the Weinberg–Tomozawa theorem predicts the leading s-wave interaction strength of Goldstone bosons not only with baryon-octet but also with baryon-decuplet states.

In this Letter we explore whether the Weinberg–Tomozawa interaction of the meson–baryon-decuplet sector has the potential to dynamically generate d-wave baryon resonances. We find that the chiral dynamics predicts the existence of octet and decuplet bound states in the 'heavy' $SU(3)$ limit. Those bound states disappear once the current quark masses of QCD are sufficiently small. It should be possible to test this prediction within lattice QCD [20]. Using physical hadron masses the predicted mass spectrum is remarkably consistent with the empirical spectrum. This finding complements a corresponding result [5–9,12,18] obtained for the s-wave baryon resonances for which chiral dynamics predicts 2 degenerate octet and one singlet state that also disappear for sufficiently small current quark masses.

2. Chiral coupled-channel dynamics: the χ-BS(3) approach

The starting point is the chiral $SU(3)$ Lagrangian (see, e.g. [21]). The relevant term that encodes the prediction of Weinberg and Tomozawa [22] for the s-wave scattering lengths of Goldstone bosons with baryon-decuplet states is readily identified,

$$\mathcal{L}_{\mathrm{WT}} = \frac{3i}{8f^2}\,\mathrm{tr}\big((\bar{B}_\nu \gamma^\mu B^\nu)\cdot[\Phi, (\partial_\mu \Phi)]_-\big), \tag{1}$$

where we dropped terms that do not contribute to the on-shell scattering process at tree level. The $SU(3)$ meson and baryon fields are written in terms of their isospin symmetric components,

$$\begin{aligned}
\Phi &= \tau\cdot\pi + \alpha^\dagger\cdot K + K^\dagger\cdot\alpha + \eta\lambda_8,\\
\bar{B}\cdot B &= \frac{1}{6}(\bar{\Delta}\mathcal{G}\Delta)\cdot\tau + \frac{1}{6}\bar{\Delta}\cdot\Delta\big(2+\sqrt{3}\lambda_8\big) + \frac{1}{3}\bar{\Sigma}\cdot\Sigma - \frac{i}{3}\tau\cdot(\bar{\Sigma}\times\Sigma) + \frac{1}{6}\bar{\Xi}\,\Xi\big(2-\sqrt{3}\lambda_8\big)\\
&\quad + \frac{1}{6}(\bar{\Xi}\sigma\Xi)\tau + \frac{1}{3}\bar{\Omega}^-\Omega^-\big(1-\sqrt{3}\lambda_8\big) + \frac{1}{\sqrt{6}}\bar{\Delta}(\Sigma\cdot T)\alpha + \frac{1}{\sqrt{6}}\alpha^\dagger\big(\bar{\Sigma}\cdot T^\dagger\big)\Delta\\
&\quad - \frac{1}{3}\bar{\Sigma}\big(\Xi^t i\sigma_2\sigma\alpha\big) + \frac{1}{3}\big(\alpha^\dagger\sigma i\sigma_2\bar{\Xi}^t\big)\Sigma + \frac{1}{\sqrt{6}}\bar{\Omega}^-(\alpha^\dagger\cdot\Xi) + \frac{1}{\sqrt{6}}(\bar{\Xi}\cdot\alpha)\Omega^-,
\end{aligned} \tag{2}$$

with the Gell-Mann matrices, λ_i, and the isospin doublet fields $K = (K^+, K^0)^t$ and $\Xi = (\Xi^0, \Xi^-)^t$. The isospin Pauli matrices $\sigma = (\sigma_1, \sigma_2, \sigma_3)$ act exclusively in the space of isospin doublet fields (K, N, Ξ) and the matrix-valued isospin doublet α,

$$\begin{aligned}
&\alpha^\dagger = \frac{1}{\sqrt{2}}(\lambda_4 + i\lambda_5, \lambda_6 + i\lambda_7), \qquad \tau = (\lambda_1, \lambda_2, \lambda_3),\\
&\mathcal{G}_i = 3\vec{T}\tau_i\vec{T}^\dagger, \qquad \vec{T}\cdot\vec{T}^\dagger = 1, \qquad T_i^\dagger T_j = \delta_{ij} - \frac{1}{3}\sigma_i\sigma_j.
\end{aligned} \tag{3}$$

The 4×2 matrices T_j in (3) describe the transition from isospin-$\frac{1}{2}$ to $\frac{3}{2}$ states. The scattering process is described by the amplitudes that follow as solutions of the coupled-channel Bethe–Salpeter equation,

$$\begin{aligned}
T_{\mu\nu}(\bar{k}, k; w) &= K_{\mu\nu}(\bar{k}, k; w) + \int \frac{d^4 l}{(2\pi)4} K_{\mu\alpha}(\bar{k}, l; w) G_{\alpha\beta}(l; w) T_{\beta\nu}(l, k; w),\\
G_{\mu\nu}(l; w) &= -i D\big(\tfrac{1}{2}w - l\big) S_{\mu\nu}\big(\tfrac{1}{2}w + l\big),
\end{aligned} \tag{4}$$

Table 1
The column $R_\mu^{(I,S)}(q,p)$ for isospin (I) and strangeness (S)

$(\frac{1}{2},-4)$	$(0,-3)$	$(1,-3)$	$(\frac{1}{2},-2)$
$(\bar K\Omega^\mu)$	$\begin{pmatrix}(\frac{1}{\sqrt2}\bar K\Xi^\mu)\\(\eta\Omega^\mu)\end{pmatrix}$	$\begin{pmatrix}(\pi\Omega^\mu)\\(\frac{1}{\sqrt2}\bar K\sigma\Xi^\mu)\end{pmatrix}$	$\begin{pmatrix}(\frac{1}{\sqrt3}\pi\cdot\sigma\Xi^\mu)\\(\frac{i}{\sqrt3}\Sigma^\mu\cdot\sigma\sigma_2\bar K^t)\\(\eta\Xi^\mu)\\(K\Omega^\mu)\end{pmatrix}$
$(\frac{3}{2},-2)$	$(0,-1)$	$(1,-1)$	$(2,-1)$
$\begin{pmatrix}(\pi\cdot T\Xi^\mu)\\(\Sigma^\mu\cdot T i\sigma_2\bar K^t)\end{pmatrix}$	$\begin{pmatrix}(\frac{1}{\sqrt3}\pi\cdot\Sigma^\mu)\\(\frac{1}{\sqrt2}K^t i\sigma_2\Xi^\mu)\end{pmatrix}$	$\begin{pmatrix}(\frac{-i}{\sqrt2}\pi\times\Sigma^\mu)\\(\sqrt{\frac{3}{4}}\bar K\vec T^\dagger\Delta^\mu)\\(\eta\Sigma^\mu)\\(\frac{1}{\sqrt2}K^t i\sigma_2\sigma\Xi^\mu)\end{pmatrix}$	$\begin{pmatrix}\frac12(\pi_i\Sigma_j^\mu+\pi_j\Sigma_i^\mu)-\frac13\delta_{ij}\pi\cdot\Sigma^\mu\\\frac{1}{\sqrt8}\bar K(\sigma_i T_j^\dagger+\sigma_j T_i^\dagger)\Delta^\mu\end{pmatrix}$
$(\frac{1}{2},0)$	$(\frac{3}{2},0)$	$(\frac{5}{2},0)$	
$\begin{pmatrix}(\frac{1}{\sqrt2}\pi\cdot T^\dagger\Delta^\mu)\\(\frac{1}{\sqrt3}\Sigma^\mu\cdot\sigma K)\end{pmatrix}$	$\begin{pmatrix}(\frac{1}{\sqrt{15}}\pi\cdot\mathcal{G}\Delta^\mu)\\(\eta\Delta^\mu)\\(\Sigma^\mu T K)\end{pmatrix}$	$((\frac12(\pi_i T_j^\dagger+\pi_j T_i^\dagger)-\frac13\delta_{ij}\pi\cdot T^\dagger)\Delta^\mu)$	
$(1,1)$		$(2,1)$	
$(\sqrt{\frac34}K^t i\sigma_2\vec T^\dagger\Delta^\mu)$		$(\frac{1}{\sqrt8}K^t i\sigma_2(\sigma_i T_j^\dagger+\sigma_j T_i^\dagger)\Delta^\mu)$	

where we suppress the coupled-channel structure for simplicity. The meson and decuplet propagators, $D(q)$ and $S_{\mu\nu}(p)$, are used in the notation of [3]. The scattering amplitude $T_{\mu\nu}(\bar k,k;w)$ decouples into various sectors characterized by isospin (I) and strangeness (S) quantum numbers. This decomposition follows from a corresponding one (see [3]) of the interaction Lagrangian,

$$\mathcal{L}_{\rm WT}(\bar k,k;w)=\sum_{I,S}R_\mu^{(I,S)\dagger}(\bar q,\bar p)\gamma_0 g^{\mu\alpha}K_{\alpha\beta}^{(I,S)}(\bar k,k;w)g^{\beta\nu}R_\nu^{(I,S)}(q,p), \tag{5}$$

where the column $R^{(I,S)}(q,p)$ specifies our phase convention for the isospin states. We introduced convenient kinematics:

$$w=p+q=\bar p+\bar q,\qquad k=\frac12(p-q),\qquad \bar k=\frac12(\bar p-\bar q), \tag{6}$$

where $q,p,\bar q,\bar p$ are the initial and final meson and baryon 4-momenta. In Table 1 we collect $R^{(I,S)}(q,p)$ for all isospin and strangeness channels considered in this work. Following the χ-BS(3) approach developed in [2,3] the interaction kernel is decomposed into a set of covariant projectors that have well defined total angular momentum, J, and parity, P,

$$K_{\mu\nu}(\bar k,k;w)=\sum_{J,P}K^{(J,P)}(\sqrt s)\mathcal{Y}_{\mu\nu}^{(J,P)}(\bar q,q,w),$$

$$\mathcal{Y}_{\mu\nu}^{(1/2,\pm)}(\bar q,q;w)=\frac16\left(\gamma_\mu-\frac{w_\mu}{w^2}\not w\right)\left(\mp1-\frac{\not w}{\sqrt{w^2}}\right)\left(\gamma_\nu-\frac{w_\nu}{w^2}\not w\right),$$

$$\mathcal{Y}^{(3/2,\pm)}_{\mu\nu}(\bar q, q; w) = \frac{1}{2}\left(g_{\mu\nu} - \frac{w_\mu w_\nu}{w^2}\right)\left(\mp 1 + \frac{\not w}{\sqrt{w^2}}\right) - \frac{1}{6}\left(\gamma_\mu - \frac{w_\mu}{w^2}\not w\right)\left(\mp 1 - \frac{\not w}{\sqrt{w^2}}\right)\left(\gamma_\nu - \frac{w_\nu}{w^2}\not w\right), \quad (7)$$

where we provide the projector, $\mathcal{Y}^{(1/2,\pm)}_{\mu\nu}(\bar q, q; w)$ describing p- and d-wave scattering with $J = 1/2$ and $\mathcal{Y}^{(3/2,\pm)}_{\mu\nu}(\bar q, q; w)$ relevant for s-and p-wave scattering with $J = 3/2$. The merit of the projectors is that they decouple the Bethe–Salpeter equation (4) into orthogonal sectors labelled by the total angular momentum J. Here we suppress an additional matrix structure that follows since for given parity and total angular momentum, $J \geqslant 3/2$, two distinct angular momentum states couple. In general, for given J, the projector form a 2×2 matrix, for which we displayed in (7) only its leading 11-component. The effect of the remaining components is phase-space suppressed and not considered here. Referring to the detailed discussion given in [2] we assume a systematic on-shell reduction of an effective interaction kernel,

$$V = K + \mathcal{O}\big(Q^3\big),$$

which is expanded according to chiral power counting rules. In addition, we insist on the renormalization condition,

$$T^{(I,S)}_{\mu\nu}(\bar k, k; w)\big|_{\sqrt{s}=\mu(I,S)} = V^{(I,S)}_{\mu\nu}(\bar k, k; w)\big|_{\sqrt{s}=\mu(I,S)}, \quad (8)$$

that complies with approximate crossing symmetry. For the subtraction points, $\mu(I, S)$, the natural choices are determined by the baryon octet masses,

$$\mu(I,+1) = \mu(I,-3) = \frac{1}{2}(m_\Lambda + m_\Sigma), \qquad \mu(I,0) = m_N,$$
$$\mu(0,-1) = m_\Lambda, \qquad \mu(1,-1) = m_\Sigma, \qquad \mu(I,-2) = \mu(I,-4) = m_\Xi, \quad (9)$$

as explained in detail in [2]. The renormalization condition reflects the basic assumption our effective field theory is based on, namely, that at subthreshold energies the scattering amplitudes can be evaluated in standard chiral perturbation theory with the typical expansion parameter $m_K/(4\pi f) < 1$ with $f \simeq 90$ MeV. Once the available energy is sufficiently high to permit elastic two-body scattering a further typical dimensionless parameter $m_K^2/(8\pi f^2) \sim 1$ arises. Since this ratio is uniquely linked to two-particle reducible diagrams it is sufficient to sum those diagrams keeping the perturbative expansion of all irreducible diagrams. This is achieved by (4). The subtraction points (9) are the unique choices that protect the s-channel baryon-octet masses manifestly in the p-wave $J = 1/2$ scattering amplitudes. The merit of the scheme [1,2,11] lies in the property that, for instance, the $K\Xi$ and $\bar K\Xi$ scattering amplitudes match at $\sqrt{s} \sim m_\Xi$ approximately as expected from crossing symmetry. In [2] we suggested to match s- and u-channel unitarized scattering amplitudes at subthreshold energies. This construction reflects our basic assumption that diagrams showing an s-channel or u-channel unitarity cut need to be summed to all orders at least at energies close to where the diagrams develop their imaginary part. By construction, a matched scattering amplitude satisfies crossing symmetry exactly at energies where the scattering process takes place. At subthreshold energies crossing symmetry is implemented approximatively only, however, to higher and higher accuracy when more chiral correction terms are considered. Insisting on the renormalization condition (8), (9) guarantees that subthreshold amplitudes match smoothly and therefore the final 'matched' amplitude complies with the crossing-symmetry constraint to high accuracy. The natural subtraction points (9) can also be derived if one incorporates photon–baryon inelastic channels. Then additional constraints arise. For instance, the reaction $\gamma\Xi \to \gamma\Xi$, which is subject to a crossing symmetry constraint at threshold, may go via the intermediate states $\bar K\Lambda$ or $\bar K\Sigma$. Here we assume that this reaction is described by a coupled-channel scattering equation (4) where the effective on-shell interaction kernel V is expanded in chiral perturbation theory.

Given the subtraction scales (9) a leading-order calculation within the χ-BS(3) approach is parameter free. Of course, chiral correction terms do lead to further so far unknown parameters which need to be adjusted to data. Within the χ-BS(3) approach such correction terms enter the effective interaction kernel V rather than leading to subtraction scales different from (9) as it is assumed in [16–18]. In particular, the leading correction effects are determined by the counter terms of chiral order Q^2. The effect of altering the subtraction scales away from their optimal values (9) can be compensated for by incorporating counter terms in the chiral Lagrangian that carry order Q^3. Our effective field theory is based on the assumption that the scattering amplitudes are perturbative at subthreshold energies. The latter is not necessarily true in the scheme applied in [16–18], which may be viewed as promoting the counter terms of chiral order Q^3 to be unnaturally large. If the subtraction scales are chosen far away from their natural values (9) the resulting loop functions are in conflict with chiral power counting rules [11]. Though unnaturally large Q^3 counter terms cannot be excluded from first principals one should check such an assumption by studying corrections terms systematically. A detailed test of the naturalness of the Q^3 counter terms was performed within the χ-BS(3) scheme [2] demonstrating good convergence in the channels studied without any need for promoting the counter terms of order Q^3. Possible correction terms in the approach followed in [16–18] have so far not been studied systematically for meson–baryon scattering. Moreover, if the scheme advocated in [16–18] were applied in all eleven isospin strangeness sectors with $J^P = \frac{1}{2}^-$ a total number of 26 subtraction parameters arise. This should be compared with the only ten counter terms of chiral order Q^3 contributing to the on-shell scattering amplitude at that order [2]. Selecting only the operators that are leading in the large-N_c limit of QCD out of the ten Q^3 operators only four survive [2]. We conclude that it would be inconsistent to apply the approach used in [16–18] in all isospin strangeness channels without addressing the above mismatch of parameters. Our scheme has the advantage over the one in [16–18] that once the parameters describing subleading effects are determined in a subset of sectors one has immediate predictions for all sectors (I, S). A mismatch of the number of parameters is avoided altogether since the Q^3 counter terms enter the effective interaction kernel directly.

With the decomposition (7) the solution of the Bethe–Salpeter equation takes the form

$$T_{\mu\nu}(\bar{k}, k; w) = \sum_{J,P} M^{(J,P)}(\sqrt{s})\,\mathcal{Y}^{(J,P)}_{\mu\nu}(\bar{q}, q; w),$$
$$M^{(J,P)}(\sqrt{s}) = \left[1 - K^{(J,P)}(\sqrt{s})\,J^{(J,P)}(\sqrt{s})\right]^{-1} K^{(J,P)}(\sqrt{s}), \tag{10}$$

where the loop matrix $J^{(J,P)}_{ab}(\sqrt{s})$ is diagonal in the coupled-channel space. Diagonal elements are fully specified in terms of the meson and baryon decuplet masses m and M entering the considered channel and a universal subtraction point $\mu = \mu(I, S)$ depending only on the isospin and strangeness quantum numbers. For the loop functions of the different sectors with $J^P = \frac{1}{2}^\pm, \frac{3}{2}^\pm$ we find

$$J^{(J,P)}(\sqrt{s}) = N^{(J,P)}(\sqrt{s})\left(I(\sqrt{s}) - I(\mu)\right),$$
$$I(\sqrt{s}) = \frac{1}{16\pi^2}\left(\frac{p_{\rm cm}}{\sqrt{s}}\left(\ln\left(1 - \frac{s - 2p_{\rm cm}\sqrt{s}}{m^2 + M^2}\right) - \ln\left(1 - \frac{s + 2p_{\rm cm}\sqrt{s}}{m^2 + M^2}\right)\right) + \left(\frac{1}{2}\frac{m^2 + M^2}{m^2 - M^2} - \frac{m^2 - M^2}{2s}\right)\ln\left(\frac{m^2}{M^2}\right) + 1\right) + I(0), \tag{11}$$

where

$$\sqrt{s} = \sqrt{M^2 + p^2_{\rm cm}} + \sqrt{m^2 + p^2_{\rm cm}}, \qquad E = \sqrt{M^2 + p^2_{\rm cm}},$$
$$N^{(1/2,\pm)}(\sqrt{s}) = (E \mp M)\left(\frac{2}{9}\frac{E^2}{M^2} - \frac{2}{9}\right), \qquad N^{(3/2,\pm)}(\sqrt{s}) = (E \mp M)\left(\frac{5}{9} + \frac{2}{9}\frac{E}{M} + \frac{2}{9}\frac{E^2}{M^2}\right). \tag{12}$$

It is left to identify the interaction kernel $K^{(J,P,I,S)}_{ab}(\sqrt{s})$ as predicted by the Weinberg–Tomozawa term (1). The coupled-channel structure is made explicit, with a and b referring to initial and final states,

$$K^{(\frac{1}{2},\pm,I,S)}_{ab}(\sqrt{s}) = \frac{C^{(I,S)}_{ab}}{4f^2}\left(2\sqrt{s} \mp M_a \mp M_b\right), \qquad K^{(\frac{3}{2},\pm,I,S)}_{ab}(\sqrt{s}) = \frac{C^{(I,S)}_{ab}}{4f^2}\left(2\sqrt{s} \pm M_a \pm M_b\right), \tag{13}$$

Table 2
The coefficients $C^{(I,S)}$ of the Weinberg–Tomozawa term that characterize the meson–baryon-decuplet interaction introduced in (13). The ordering of the states is introduced in Table 1

(I,S)	11	12	22	13	23	33	14	24	34	44
$(\frac{1}{2},-4)$	-3	–	–	–	–	–	–	–	–	–
$(0,-3)$	0	-3	0	–	–	–	–	–	–	–
$(1,-3)$	0	$-\sqrt{3}$	-2	–	–	–	–	–	–	–
$(\frac{1}{2},-2)$	2	-1	2	0	-3	0	$\frac{3}{\sqrt{2}}$	0	$\frac{3}{\sqrt{2}}$	3
$(\frac{3}{2},-2)$	-1	2	-1	–	–	–	–	–	–	–
$(0,-1)$	4	$\sqrt{6}$	3	–	–	–	–	–	–	–
$(1,-1)$	2	1	4	0	$-\sqrt{6}$	0	2	0	$-\sqrt{6}$	1
$(2,-1)$	-2	$\sqrt{3}$	0	–	–	–	–	–	–	–
$(\frac{1}{2},0)$	5	-2	2	–	–	–	–	–	–	–
$(\frac{3}{2},0)$	2	0	0	$\sqrt{\frac{5}{2}}$	$\frac{3}{\sqrt{2}}$	-1	–	–	–	–
$(\frac{5}{2},0)$	-3	–	–	–	–	–	–	–	–	–
$(1,1)$	1	–	–	–	–	–	–	–	–	–
$(2,1)$	-3	–	–	–	–	–	–	–	–	–

and M_a and M_b denoting the isospin averaged decuplet masses of initial and final channel. The interaction kernels are identical for the two channels, $J = 1/2$ and $J = 3/2$, considered here. The '$\pm$' in (13) keeps track of the parity quantum number with $P = \pm 1$. The values for the coefficient matrix $C_{ab}^{(I,S)}$ characterizing the strength of the Weinberg–Tomozawa term in the coupled-channel space are collected in Table 2. A remark of caution is in order here. Though we provide here the contribution of the Weinberg–Tomozawa term to the leading channels, it should be emphasized that only for $J^P = \frac{3}{2}^-$ the latter term constitutes the dominant contribution to the interaction kernel. In the remaining channels there exist further terms in the chiral Lagrangian, so far basically unknown, that may change the interaction kernel significantly. Nevertheless, it is instructive to study the consequence of the Weinberg–Tomozawa term in those channels as it is. One may draw qualitative conclusion as to whether the chiral Lagrangian has the potential to dynamically generate $J^P = \frac{3}{2}^+$ and $J^P = \frac{1}{2}^\pm$ baryon resonances as well.

3. Results

In order to study the formation of baryon resonances we generate speed plots as suggested by Höhler [23]. The speed $\mathrm{Speed}_{ab}^{(J,P)}(\sqrt{s}\,)$ of a given channel ab is introduced by [23,24],

$$t_{ab}^{(J,P)}(\sqrt{s}\,) = \frac{1}{8\pi\sqrt{s}}\big(p_{\mathrm{cm}}^{(a)} N_a^{(I,P)}(\sqrt{s}\,)\, p_{\mathrm{cm}}^{(b)} N_b^{(I,P)}(\sqrt{s}\,)\big)^{1/2} M_{ab}^{(I,P)}(\sqrt{s}\,),$$

$$\mathrm{Speed}_{ab}^{(J,P)}(\sqrt{s}\,) = \left|\sum_c \left[\frac{d}{d\sqrt{s}} t_{ac}^{(I,P)}(\sqrt{s}\,)\right]\big(\delta_{cb} + 2i\, t_{cb}^{(I,P)}(\sqrt{s}\,)\big)^\dagger\right|. \tag{14}$$

If a resonance with not too large decay width sits in the amplitude $M^{(I,P)}(\sqrt{s}\,)$ a clear peak structure emerges in the speed plot even if the resonance structure is masked by a background phase.

We begin with a discussion of our results in the $SU(3)$ limit. The latter is not defined uniquely depending on the magnitude of the current quark masses, $m_u = m_d = m_s$. We study this dependence at chiral order Q^2. Using the meson–baryon sigma terms of [2] a meson mass $m_{[8]} \simeq m_K$ implies, for instance, a baryon octet mass $M_{[8]} \simeq 1270$ MeV. Applying the large-N_c limit one may use $M_{[8]} = M_{[10]}$ for the baryon-decuplet masses. This

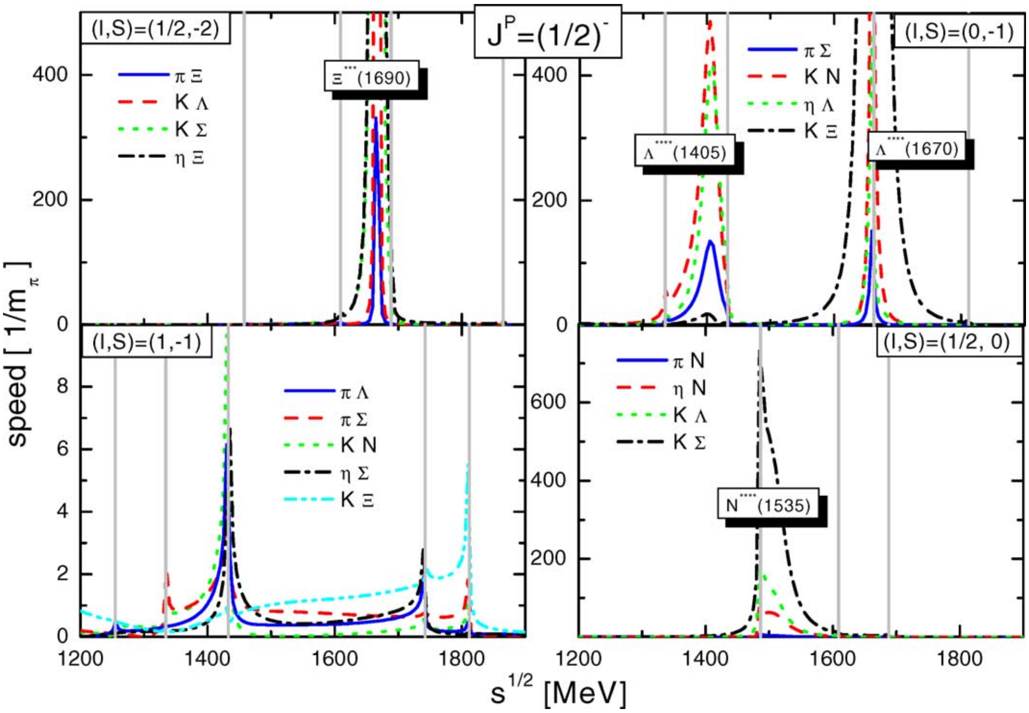

Fig. 1. Diagonal speed plots of the $J^P = \frac{1}{2}^-$ sector. The vertical lines show the opening of inelastic meson–baryon-decuplet channels. Parameter free results are obtained in terms of physical masses and $f = 90$ MeV [12].

scenario we call the 'heavy' $SU(3)$ limit. Similarly, we introduce the notion of a 'light' $SU(3)$ limit with $m_{[8]} = m_\pi$ and $M_{[8]} \simeq 860$ MeV. Note that in the two scenarios the subtraction scales of (9) is $\mu = M_{[8]}$.

Before discussing our results for meson–baryon-decuplet scattering we briefly recall the results of the recent work [12] which addressed the chiral dynamics of s-wave meson–baryon-octet states. In the $SU(3)$ limit meson–baryon-octet scattering is classified according to

$$8 \otimes 8 = 27 \oplus \overline{10} \oplus 10 \oplus 8 \oplus 8 \oplus 1. \tag{15}$$

The Weinberg and Tomozawa interaction predicts attraction in the two 8-plet and the 1-plet channel but repulsion in the 27-plet channel [18]. The repulsion in the 27-plet channels follows, for instance, from the negative signs of the coefficients $C^{(I,S)}$ in the $(1,1)$ and $(2,-1)$ sectors that involve one channel only (see, e.g., [2]). All together the 27-plet has contributions in nine channels with

$$(I,S)_{[27]} = (1,1),\ \left(\tfrac{3}{2},0\right),\ \left(\tfrac{1}{2},0\right),\ (2,-1),\ (1,-1),\ (0,-1),\ \left(\tfrac{3}{2},-2\right),\ \left(\tfrac{1}{2},-2\right),\ (1,-3).$$

Similarly, the $\overline{10}$-plet and 10-plet contribute in

$$(I,S)_{[\overline{10}]} = (0,1),\ \left(\tfrac{1}{2},0\right),\ (1,-1),\ \left(\tfrac{3}{2},-2\right), \qquad (I,S)_{[10]} = \left(\tfrac{3}{2},0\right),\ (1,-1),\ \left(\tfrac{3}{2},-2\right),\ (0,-3).$$

The vanishing of $C^{(0,1)}$ (see, e.g., [2]) tells that the interaction strength vanishes in the $\overline{10}$-plet channel [18]. An analogous result [18] holds for the 10-plet channel. This follows most efficiently from the vanishing of $C^{(0,-3)}$. As a consequence, in the 'heavy' $SU(3)$ limit the chiral dynamics predicts two degenerate octet bound states together with a non-degenerate singlet state [5–9,12,18]. In the 'light' $SU(3)$ limit all states disappear leaving no clear signal in any of the speed plots. Using physical meson and baryon octet masses the bound-state turn into resonances as shown in Fig. 1. The speed plots show strong evidence for the formation of the $\Xi(1690)$, $\Lambda(1405)$, $\Lambda(1670)$ and $N(1535)$ resonances. The 'disappearance' of the remaining states was discussed in detail in [12].

We turn to the meson–baryon-decuplet scattering process—the focus of this work. In the $SU(3)$ limit this process decouples into four different channels, labelled according to

$$8 \otimes 10 = 35 \oplus 27 \oplus 10 \oplus 8. \tag{16}$$

In the $J^P = \frac{3}{2}^-$ sector the Weinberg–Tomozawa interaction is attractive in the 8-plet, 10-plet and 27-plet channel, but repulsive in the 35-plet channel. Therefore, one may expect resonances or bound states in the former channels. For instance, the repulsion in the 35-plet channel with

$$(I,S)_{[35]} = (2,1),\ \left(\tfrac{5}{2},0\right),\ \left(\tfrac{3}{2},0\right),\ (2,-1),\ (1,-1),\ \left(\tfrac{3}{2},-2\right),\ \left(\tfrac{1}{2},-2\right),\ (1,-3),\ (0,-3),\ \left(\tfrac{1}{2},-4\right), \tag{17}$$

follows from the negative $C^{(I,S)}$ coefficients (see Table 2) in the $(2,1)$ and $(\frac{1}{2},-4)$ sectors. Similarly the positive $C^{(1,1)}$ coefficients reflects the weak attraction in the 27-plet channel. Indeed, in the 'heavy' $SU(3)$ limit we find $72 = 4 \times (8 + 10)$ bound states of masses 1615 and 1703 MeV in this sector forming an octet and decuplet representation of the $SU(3)$ group. This result is rather insensitive to the precise values used for the subtraction scale. For instance, increasing the latter by 200 MeV away from its natural value the octet and decuplet masses come at 1670 and 1734 MeV, respectively. Similarly, a decrease of the subtraction scale by 200 MeV leads to 1578 and 1678 MeV. Though we would argue that a change of the subtraction scale by 200 MeV is not acceptable, deteriorating the good matching properties of subthreshold amplitudes, the above numbers may nevertheless estimate a typical error band encountered in the leading-order calculation presented here. We do not find a 27-plet-bound state reflecting the weaker attraction in that channel. However, if we artificially increase the amount of attraction by about 40% by lowering the value of f in the Weinberg–Tomozawa term, a clear bound state arises in this channel also. This phenomenon persists if we use somewhat larger baryon-decuplet masses. A contrasted result is obtained if we lower the meson masses down to the pion mass arriving at the 'light' $SU(3)$ limit. Then we find neither bound nor resonance octet or decuplet states. Increasing the baryon-decuplet mass somewhat away from the baryon-octet mass does not change this result.

Even though the Weinberg–Tomozawa term does not constitute the complete leading-order interaction in the $J^P = \frac{1}{2}^\pm$ and $J^P = \frac{3}{2}^+$ channels it is nevertheless instructive to explore the consequences thereof in those sectors. Using physical masses we observe in the speed plots of the $J^P = \frac{1}{2}^+$ sector octet and decuplet resonances with masses centering around 2000 MeV. Of course, the resonances of this channel are dominated by s-wave meson–baryon-octet channels [12] and one should not expect any realistic results in terms of d-wave meson–baryon-decuplet channels only. Similarly, we do not find any clear signal of resonances in the p-wave channels $J^P = \frac{1}{2}^-$ and $J^P = \frac{3}{2}^+$ of masses below 2000 MeV.

We turn to the central result of this work. In Fig. 2 speed plots of the $J^P = \frac{3}{2}^-$ sector are shown for all channels in which octet and decuplet resonance states are expected. It is a remarkable success of the present scheme that it predicts parameter free the four star hyperon resonances $\Xi(1820)$, $\Lambda(1520)$, $\Sigma(1670)$ with masses quite close to the empirical values. The nucleon and isobar resonances $N(1520)$ and $\Delta(1700)$ also present in Fig. 1, are predicted with less accuracy. The important result here is the fact that those resonances are generated at all. It should not be expected to obtain already fully realistic results in this leading-order calculation. For instance, chiral correction terms are expected to provide a d-wave $\pi\Delta$-component of the $N(1520)$.

We continue with the peak in the $(0,-3)$-speeds at mass 1950 MeV. Since this is below all thresholds it is in fact a bound state. Such a state has so far not been observed but is associated with a decuplet resonance. It is a clear and solid prediction of our scheme and we suggest to search for such a state. Typically such a state is predicted to have resonance character in large-N_c phenomenology and quark-model calculations with a mass above 2000 MeV [19]. Further states belonging to the decuplet are seen in the $(\frac{1}{2},-2)$- and $(1,-1)$-speeds at masses 2100 and 1920 MeV. The latter state can be identified with the three star $\Xi(1940)$ resonance. Finally, we

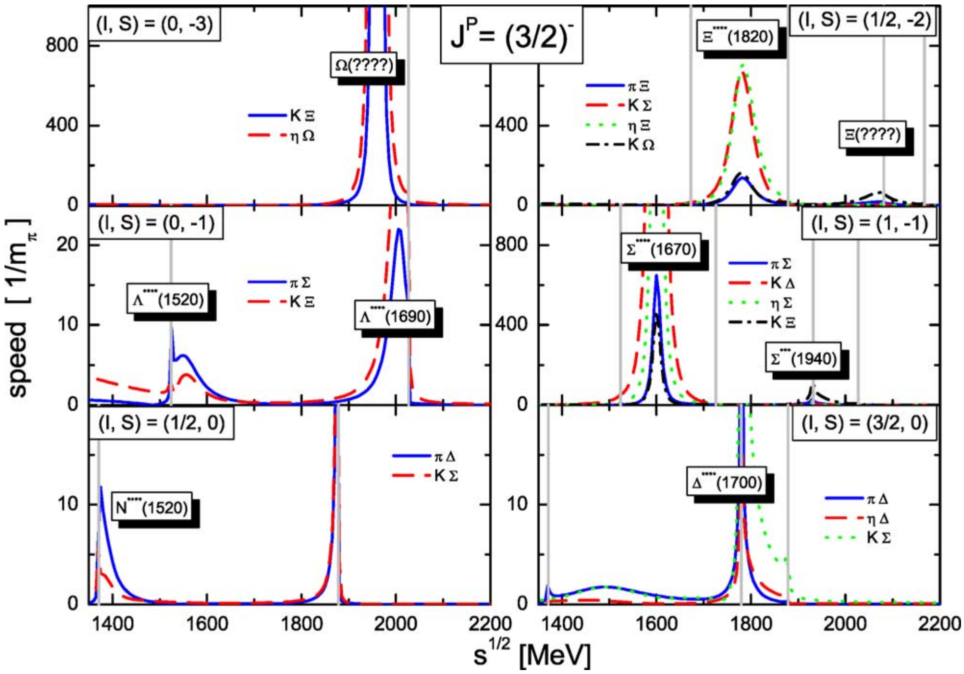

Fig. 2. Diagonal speed plots of the $J^P = \frac{3}{2}^-$ sector. The vertical lines show the opening of inelastic meson–baryon-decuplet channels. Parameter-free results are obtained in terms of physical masses and $f = 90$ MeV.

point at the fact that the $(0, -1)$-speeds show signals of two resonance states consistent with the existence of the four star resonance $\Lambda(1520)$ and $\Lambda(1690)$ even though in the 'heavy' $SU(3)$ limit we observed only one bound state. It appears that the $SU(3)$ symmetry breaking pattern generates the 'missing' state in this particular sector by promoting the weak attraction of the 27-plet contribution in (16).

It should be noted that the mass and widths parameters one may extract from the speed plots in Fig. 2 could be improved by incorporating contributions from meson–baryon-octet decays not considered here. In particular, one would expect from previous phenomenological studies like [3] that the vector-meson–baryon octet channels may play an important role in the course of improving the results of this work. One may speculate that the weak attraction found in the 27-plet channel which is almost strong enough to generate resonance structures could generate states with anomalous quantum numbers like $(I, S) = (1, 1)$ if the correction terms conspire to slightly increase the attraction found already at leading order.

Acknowledgements

The authors thank the ECT* (Trento) for hospitality and pleasant working conditions. E.K. acknowledges partial support from GSI.

References

[1] M.F.M. Lutz, E.E. Kolomeitsev, Found. Phys. 31 (2001) 1671.
[2] M.F.M. Lutz, E.E. Kolomeitsev, Nucl. Phys. A 700 (2002) 193.
[3] M.F.M. Lutz, Gy. Wolf, B. Friman, Nucl. Phys. A 706 (2002) 431.

[4] M.F.M. Lutz, GSI-Habil-2002-1.
[5] H.W. Wyld, Phys. Rev. 155 (1967) 1649.
[6] R.H. Dalitz, T.C. Wong, G. Rajasekaran, Phys. Rev. 153 (1967) 1617.
[7] J.S. Ball, W.R. Frazer, Phys. Rev. Lett. 7 (1961) 204.
[8] G. Rajasekaran, Phys. Rev. 5 (1972) 610.
[9] R.K. Logan, H.W. Wyld, Phys. Rev. 158 (1967) 1467.
[10] P.B. Siegel, W. Weise, Phys. Rev. C 38 (1988) 2221.
[11] M.F.M. Lutz, E.E. Kolomeitsev, in: Proc. of Int. Workshop XXVIII on Gross Properties of Nuclei and Nuclear Excitations, Hirschegg, Austria, January 16–22, 2000.
[12] C. García-Recio, M.F.M. Lutz, J. Nieves, Phys. Lett. B 548 (2004) 49.
[13] N. Kaiser, P.B. Siegel, W. Weise, Nucl. Phys. A 594 (1995) 325.
[14] J. Nieves, E. Ruiz Arriola, Phys. Rev. D 63 (2001) 076001.
[15] C. García-Recio, J. Nieves, E. Ruiz Arriola, M.J. Vicente-Vacas, Phys. Rev. D 67 (2003) 076009.
[16] A. Ramos, E. Oset, C. Bennhold, Phys. Rev. Lett. 89 (2002) 252001.
[17] E. Oset, A. Ramos, C. Bennhold, Phys. Lett. B 527 (2002) 99.
[18] D. Jido, et al., nucl-th/0303062.
[19] C.L. Schat, J.L. Goity, N.N. Scoccola, Phys. Rev. Lett. 88 (2002) 102002.
[20] D.G. Richards, in: Proc. of 'NSTAR 2002', Pittsburgh, October 2002, and references therein.
[21] A. Krause, Helv. Phys. Acta 63 (1990) 3.
[22] S. Weinberg, Phys. Rev. Lett. 17 (1966) 616;
Y. Tomozawa, Nuovo Cimento A 46 (1966) 707.
[23] G. Höhler, πN Newslett. 9 (1993) 1.
[24] F.T. Smith, Phys. Rev. 118 (1960) 349.